Quantum Electronics **39** (5) 455–462 (2009)

WAVEGUIDES

PACS numbers: 42.81.Dp; 42.81.Qb; 78.67.Ch
DOI: 10.1070/QE2009v039n05ABEH013958

Transmission of evanescent modes through a subwavelength aperture of a cylindrical waveguide. 1. Ideal metal approximation

T.I. Kuznetsova, V.S. Lebedev

***Abstract*. The transmission of an evanescence electromagnetic wave through the subwavelength aperture of a dielectric cylindrical metal-coated waveguide is studied. In the ideal metal approximation a theoretical approach to the description of the field structure in a nanowaveguide is developed, which takes into account the transformation of the initial wave reflected from the output aperture. The complex reflection coefficient of a supercritical waveguide mode from the subwavelength aperture is calculated. The dependence of the field structure at the waveguide output on the ratio of its radius to the optical wavelength and on the dielectric constants of the waveguide core and the environment is found. The conditions for the appearance of a plasmon resonance in the presence of a medium with the negative dielectric constant in front of the input hole of the waveguide are found.**

Keywords: *evanescent electromagnetic wave, cylindrical nanowaveguide, subwavelength aperture, ideal metal.*

1. Introduction

The extensive development of nanooptics is closely related to the elaboration of efficient methods for producing light waves with the subwavelength localisation [1, 2]. When working with the localised fields, new aspects are revealed in a number of representations, which seemed to be established in conventional optics. Thus, in considering the interaction of optical fields with nanostructures, such notions as light reflection, transmission, complex light flow, impedance acquire a new nuance. It also turns out that the analysis of these parameters calls for the development of a special investigation method.

In this paper, we study the specific features of localised fields by the example of the following model problem: a semi-infinite cylindrical waveguide with a circle input nanohole leading to the open half-space (Fig. 1). Similar problems associated with the light propagation through the subwavelength-sized hole have been discussed for many years in the literature. The strict investigation of this problem was initiated in paper [3], which considered the incidence of a plane wave on an infinite thin ideally-conducting screen with a small pin-hole. A more complete solution of this problem was presented in [4]. Later, papers appeared which studied a somewhat different geometry. The incidence of a light wave from the outside on the end-face of a cylindrical waveguide and on a conic waveguide was considered in papers [5] and [6], respectively. The authors of paper [7] studied the wave transmission through an open two-dimensional waveguide representing a slit tapering off at the output to an open space, the transmission of radiation through a pyramidal waveguide was investigated paper [8], and the light exit from a conic waveguide into the open space was examined in paper [9]. The incidence of the wave on the screen of finite thickness connected with a waveguide as well as the light propagation through the subwavelength circular aperture filled with a refractive medium in a metal film were considered in papers [10] and [11–15], respectively. In a number of our papers, we studied the field structure and the transmission efficiency of light by nanotapered waveguides filled with a dielectric [16–18] or semiconductor [19–22] medium.

Recall that earlier papers [3, 4], significant from the general theory point of view, were also important in the applied aspect for the problems related to microwave resonators. As for later works on the 'leakage' of radiation through a small hole, they were aimed at simulation of optical probes used in near-field microscopy. In this case, different papers simulated the variants of local illumination

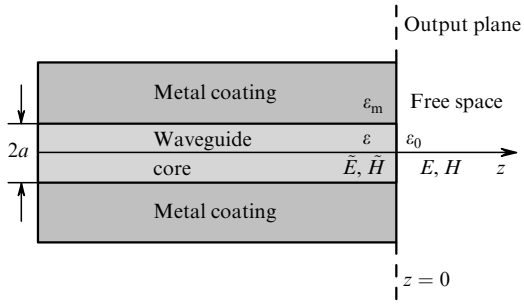

Figure 1. Schematic of the transverse cross section of a cylindrical waveguide with a metal coating: $2a$ is the diameter of the output aperture; ε, ε_m and ε_0 are dielectric constants of the waveguide core, metal walls and environment.

T.I. Kuznetsova P.N. Lebedev Physics Institute, Russian Academy of Sciences, Leninsky prosp. 53, 119991 Moscow, Russia;
e-mail: tkuzn@sci.lebedev.ru;
V.S. Lebedev P.N. Lebedev Physics Institute, Russian Academy of Sciences, Leninsky prosp. 53, 119991 Moscow, Russia; Moscow Institute of Physics and Technology (State University), Institutskii per. 9, 141700 Dolgoprudnyi, Moscow region, Russia; e-mail: vlebedev@sci.lebedev.ru

Received 12 August 2008
Kvantovaya Elektronika **39** (5) 455–462 (2009)
Translated by I.A. Ulitkin

of the object under study (illumination regime) and collection of the local response appearing upon illumination of the object by an extended source (collection regime). Different ways for realising this or that variant lead to the investigation of different geometric schemes; significantly different was also the applied mathematic method.

From the theoretical point of view, the most complex moment in such problems is the analysis of the field behaviour at the interface of the subwavelength localisation region and the microscopic region. The above papers, except for [3, 4], either paid no attention to this problem or, if it was studied as in [7], performed separate numerical calculations for a waveguide with specified parameters and at a given optical wavelength. Therefore, it was impossible to evaluate the role and the scale of the effects appearing at the interface when geometric and dielectric parameters of the scheme are varied.

Before proceeding to the statement of this paper, recall the investigations of open waveguides performed by L.A. Vainshtein [23]. At first glance, these studies are very close with respect to the formulation of the optical probe problems. However, paper [23] deals with propagating but not evanescent waves in a waveguide. In this connection, the results of paper [23] cannot be directly applied to supercritical waveguides, although it is these waveguides that are of special interest for nanooptics.

Below, we present the approach based on the developed field-conjugation method at the waveguide – free space interface. The offered method demonstrates the possibility of introducing a convenient parameter taking into account the role of the above interface, – the reflection coefficient of the initial field from the aperture. We will show below that in fact, it is sufficient to calculate the only one coefficient in order to describe with good accuracy the main parameters of the electromagnetic field inside and outside the waveguide.

2. Field characteristics in an infinite waveguide and in a free space

Let us present the general expressions determining the structure of a monochromatic electromagnetic field in a cylindrical circular waveguide. We will omit the time multiplier $\exp(-\mathrm{i}\omega t)$ and will use everywhere below cylindrical coordinates ρ, φ, z. The general expressions for the transverse-magnetic (TM_{mn}) and transverse-electric (TE_{mn}) modes of a cylindrical waveguide with ideally conducting walls can be found elsewhere in monographs [24, 25]. In the general case, it is convenient to express the fields through the electric and magnetic Hertz potentials. However, in this paper we will consider only transverse-magnetic TM_{0n} modes with the azimuth wave number $m = 0$. In this case, only three field components $\tilde{E}_\rho$, $\tilde{E}_z$ and $\tilde{H}_\varphi$ are nonzero, and we can write compact expressions for the fields without using the Hertz potential. The fields are expressed through the zero-order Bessel function $J_0(x)$ and its derivative $J_1(x)$:

$$\tilde{E}_\rho = CJ_1(q\rho)\exp\left[-z\left(q^2-\frac{\omega^2\varepsilon}{c^2}\right)^{1/2}\right], \tag{1}$$

$$E_z = q\left(q^2-\frac{\omega^2\varepsilon}{c^2}\right)^{-1/2} CJ_0(q\rho)\exp\left[-z\left(q^2-\frac{\omega^2\varepsilon}{c^2}\right)^{1/2}\right], \tag{2}$$

$$\tilde{H}_\varphi = -\frac{\mathrm{i}\omega\varepsilon}{c}\left(q^2-\frac{\omega^2\varepsilon}{c^2}\right)^{-1/2} CJ_1(q\rho) \times \exp\left[-z\left(q^2-\frac{\omega^2\varepsilon}{c^2}\right)^{1/2}\right]. \tag{3}$$

Here, $q \equiv q_n = \xi_n/a$ is the transverse wave number; ξ_n is the nth root at which the Bessel function $J_0(x)$ vanishes ($\xi_1 = 2.4048$, $\xi_2 = 5.5201$, $\xi_3 = 8.6537$, ...); a is the waveguide core radius; C is the constant; ε is the dielectric constant of the waveguide core. In the free space we will also consider transverse-magnetic fields with the angular structure as that in the waveguide. In this case, the expressions for the fields remain the same [expressions (1)–(3)], restrictions on the transverse wave numbers (which can be arbitrary) being only absent.

3. Fields in a semi-infinite cylindrical waveguide and in an open space

To give a strict description of the fields in a semi-infinite waveguide coupled to the open half-space, we should 'sew' together the fields in the waveguide and in the free space in the aperture, i.e. to achieve the equality of tangential components of the electric and magnetic fields at $z = 0$. To do this requires introducing all the transverse-magnetic waveguide modes (with $m = 0$, $n = 1, 2, 3, \ldots$) into consideration, and using the integral over the continuous set of wave numbers in the free space. In this case, the field components inside the waveguide will be set by the expressions

$$\tilde{E}_\rho = C\left\{J_1(q_1\rho)\exp\left[-z\left(q_1^2-\frac{\omega^2\varepsilon}{c^2}\right)^{1/2}\right] + \sum_{n=1}^{\infty}\alpha_n J_1(q_n\rho)\exp\left[z\left(q_n^2-\frac{\omega^2\varepsilon}{c^2}\right)^{1/2}\right]\right\}, \tag{4}$$

$$E_z = C\left\{q_1 J_0(q_1\rho)\left(q_1^2-\frac{\omega^2\varepsilon}{c^2}\right)^{-1/2}\exp\left[-z\left(q_1^2-\frac{\omega^2\varepsilon}{c^2}\right)^{1/2}\right] - \sum_{n=1}^{\infty}\alpha_n q_n J_0(q_n\rho)\left(q_n^2-\frac{\omega^2\varepsilon}{c^2}\right)^{-1/2} \times \exp\left[z\left(q_n^2-\frac{\omega^2\varepsilon}{c^2}\right)^{1/2}\right]\right\}, \tag{5}$$

$$\tilde{H}_\varphi = -\mathrm{i}\frac{\omega}{c}\varepsilon C\left\{J_1(q_1\rho)\left(q_1^2-\frac{\omega^2\varepsilon}{c^2}\right)^{-1/2} \times \exp\left[-z\left(q_1^2-\frac{\omega^2\varepsilon}{c^2}\right)^{1/2}\right] - \sum_{n=1}^{\infty}\alpha_n J_1(q_n\rho)\left(q_n^2-\frac{\omega^2\varepsilon}{c^2}\right)^{-1/2} \times \exp\left[z\left(q_n^2-\frac{\omega^2\varepsilon}{c^2}\right)^{1/2}\right]\right\}, \tag{6}$$

where α_n is the transformation coefficient of the initial mode to the mode with the subscript n. The expressions for the fields outside the waveguide have the form of integrals over the transverse wave numbers $\varkappa$:

$$E_\rho = \int_0^\infty \exp\left[\mathrm{i}z\left(\frac{\omega^2\varepsilon_0}{c^2} - \varkappa^2\right)^{1/2}\right] J_1(\varkappa\rho)B(\varkappa)\varkappa \mathrm{d}\varkappa, \quad (7)$$

$$E_z = \int_0^\infty \exp\left[\mathrm{i}z\left(\frac{\omega^2\varepsilon_0}{c^2} - \varkappa^2\right)^{1/2}\right] \frac{\varkappa J_0(\varkappa\rho)B(\varkappa)}{\gamma(\varkappa)} \varkappa \mathrm{d}\varkappa, \quad (8)$$

$$H_\varphi = -\mathrm{i}\,\frac{\omega\varepsilon_0}{c}\int_0^\infty \exp\left[\mathrm{i}z\left(\frac{\omega^2\varepsilon_0}{c^2} - \varkappa^2\right)^{1/2}\right] \frac{J_1(\varkappa\rho)B(\varkappa)}{\gamma(\varkappa)} \varkappa \mathrm{d}\varkappa\,. \quad (9)$$

Here,

$$\gamma(\varkappa) = \begin{cases} -\mathrm{i}\left(\dfrac{\omega^2\varepsilon_0}{c^2} - \varkappa^2\right)^{1/2} & \text{for } \dfrac{\omega^2\varepsilon_0}{c^2} > \varkappa^2, \\ \left(\varkappa^2 - \dfrac{\omega^2\varepsilon_0}{c^2}\right)^{1/2} & \text{for } \dfrac{\omega^2\varepsilon_0}{c^2} \leqslant \varkappa^2; \end{cases} \quad (10)$$

$B(\varkappa)$ is the expansion coefficient. Thus, we deal with two sets of expressions for the fields: for the inside waveguide region and for the outside region. These formally different expressions should be matched so that standard boundary conditions be fulfilled in the input hole plane.

4. Field matching at the waveguide – free space interface

For the modes under study, the boundary conditions have the form

$$E_\rho(\rho,0) = \tilde{E}_\rho(\rho,0),\ H_\varphi(\rho,0) = \tilde{H}_\varphi(\rho,0)\ \ (\rho < a). \quad (11)$$

We will assume that an ideally-conducting flange stretching from $\rho = a$ to $\rho = \infty$ is connected to the output hole of the waveguide and will consider that $E_\rho = 0$ at the flange surface.

We will substitute now $z = 0$ into expressions (4) and (7) for the components $\tilde{E}_\rho(\rho, z)$ and $E_\rho(\rho, z)$ and will require the first of boundary conditions (11) be fulfilled. In this case, we obtain the expression of the Fourier – Bessel expansion coefficients of the fields in the external space:

$$B(\varkappa) = C\sum_{n=1}^{\infty}(\delta_{n1} + \alpha_n)b_n(\varkappa). \quad (12)$$

Here, we used the expression

$$J_1(q_n\rho)\theta(\alpha - \rho) = \int_0^\infty b_n(\varkappa)J_1(\varkappa\rho)\varkappa \mathrm{d}\varkappa, \quad (13)$$

where the coefficients b_n are expressed through integrals:

$$b_n(\varkappa) = \int_0^a J_1(q_n\rho)J_1(\varkappa\rho)\rho \mathrm{d}\rho = J_1(q_n a)\,\frac{\varkappa a J_0(\varkappa a)}{q_n^2 - \varkappa^2}; \quad (14)$$

$\theta(a - \rho)$ is the step Heaviside function [$\theta(a - \rho) = 0$ at $a > \rho$ and $\theta(a - \rho) = 1$ at $\rho \leqslant a$]. Taking into account the selected values of q_n, integration in (14) yields the reduced expression for $b_n(\varkappa)$. Now we can write expression (9) for H_φ in the form

$$H_\varphi(\rho,0) = -\mathrm{i}\,\frac{\omega\varepsilon_0}{c}\,C\int_0^\infty \frac{1}{\gamma(\varkappa)}\times$$

$$\times \sum_{n=1}^{\infty}(\delta_{n1} + \alpha_n)b_n(\varkappa)J_1(\varkappa\rho)\varkappa \mathrm{d}\varkappa. \quad (15)$$

By substituting (15) into the second boundary condition from (11), we obtain

$$\varepsilon\sum_{n=1}^{\infty}(\delta_{n1} - \alpha_n)\left(q_n^2 - \frac{\omega^2\varepsilon}{c^2}\right)^{-1/2} J_1(q_n\rho)$$

$$= \varepsilon_0\int_0^\infty \frac{1}{\gamma(\varkappa)}\sum_{n=1}^{\infty}(\delta_{n1} + \alpha_n)b_n(\varkappa)J_1(\varkappa\rho)\varkappa \mathrm{d}\varkappa. \quad (16)$$

Then, we multiply both parts of equation (16) by the factor $J_1(q_p\rho)$ and integrate in $\rho\mathrm{d}\rho$ in the range from 0 to a. Note that the Bessel function for unequal values of n and p are orthogonal because they are eigenfunctions of the boundary problem of the third kind (meet the first-order Bessel equation and the boundary condition $\partial\psi/\partial\rho + a^{-1}\psi = 0$ at $\rho = a$). Taking into account the orthogonality of the functions after integration, we obtain

$$\varepsilon\,(\delta_{p1} - \alpha_p)\left(q_p^2 - \frac{\omega^2\varepsilon}{c^2}\right)^{-1/2}\int_0^a J_1^2(q_p\rho)\rho \mathrm{d}\rho$$

$$= \varepsilon_0\sum_{n=1}^{\infty}(\delta_{n1} + \alpha_n)\int_0^a J_1(q_p\rho)\rho \mathrm{d}\rho\int_0^\infty b_n(\varkappa)J_1(\varkappa\rho)\frac{\varkappa}{\gamma(\varkappa)}\,\mathrm{d}\varkappa. \quad (17)$$

We will change the integration order in the right-hand side of expression (17) and then, will use relation (14) for coefficients b_n and the expression for the integral in the left-hand side of (17):

$$\int_0^a J_1^2(q_n\rho)\rho \mathrm{d}\rho = \frac{a^2}{2}\,J_1^2(q_n a), \quad (18)$$

which is valid due to the fact that in our case, the condition $J_0(q_n a) = 0$ is fulfilled. As a result, we obtain the exact system of equations to determine the coefficients α_p at evanescent modes appearing due to the transformation of the initial TM_{01} mode:

$$\varepsilon\,(\delta_{p1} - \alpha_p)\left(q_p^2 a^2 - a^2\,\frac{\omega^2\varepsilon}{c^2}\right)^{-1/2}$$

$$= 2\varepsilon_0\sum_{n=1}^{\infty}(\delta_{n1} + \alpha_n)\,\frac{J_1(q_n a)}{J_1(q_p a)}\,I_{np}. \quad (19)$$

The real and imaginary parts of the integral $I_{np} = \mathrm{Re}\,I_{np} + \mathrm{i}\,\mathrm{Im}\,I_{np}$ in (19) are given by the expressions

$$\mathrm{Re}\,I_{np} = \int_{\varepsilon_0^{1/2}\omega a/c}^\infty \frac{[xJ_0(x)]^2}{(q_n^2 a^2 - x^2)(q_p^2 a^2 - x^2)}$$

$$\times\, x\left(x^2 - a^2\,\frac{\omega^2\varepsilon_0}{c^2}\right)^{-1/2}\mathrm{d}x, \quad (20)$$

$$\mathrm{Im}\,I_{np} = \int_0^{\varepsilon_0^{1/2}\omega a/c} \frac{[xJ_0(x)]^2}{(q_n^2 a^2 - x^2)(q_p^2 a^2 - x^2)}$$

$$\times\, x\left(a^2\,\frac{\omega^2\varepsilon_0}{c^2} - x^2\right)^{-1/2}\mathrm{d}x. \quad (21)$$

Expressions (20) and (21) play a key role in calculation of reflection and transmission of waves in the waveguide with a subwavelength-sized output hole. Note that at $ka < 1$ ($k = \omega\varepsilon_0^{1/2}/c$ is the wave number), the absolute values of the integrals I_{np} satisfy the relation $|I_{np}| \ll |I_{nn}|$ at $n \neq p$. In addition, the imaginary parts of the integrals I_{np} are markedly lower than the real parts ($\mathrm{Im}\, I_{np} \ll \mathrm{Re}\, I_{np}$). At $n = p$, we deal with asymptotic expressions

$$\mathrm{Im}\, I_{nn} = \frac{2}{3\xi_n^4}(ka)^3 \qquad (ka \ll 1), \tag{22}$$

and the absolute value of the integral I_{nn} can yield an approximate estimate:

$$|I_{nn}| \approx \left[2\left(q_n^2 a^2 - a^2\frac{\omega^2\varepsilon_0}{c^2}\right)^{1/2}\right]^{-1}. \tag{23}$$

The exact values of $\mathrm{Re}\, I_{nn}$ and $\mathrm{Im}\, I_{nn}$ are calculated numerically, because they are used to obtain the following results.

5. Construction of a solution

Let us construct the solution of system of equations (19). To obtain the first approximation to the solution, we will use the system of equations in which all the nondiagonal elements I_{np} ($n \neq p$) are replaced by zeros. It follows from this system that

$$(1-\alpha_1)\varepsilon\left(q_1^2 a^2 - a^2\frac{\omega^2\varepsilon}{c^2}\right)^{-1/2} = 2\varepsilon_0(1+\alpha_1)I_{11}, \tag{24}$$

$$-\alpha_p\varepsilon\left(q_p^2 a^2 - a^2\frac{\omega^2\varepsilon}{c^2}\right)^{-1/2} = 2\varepsilon_0\alpha_p I_{pp}. \tag{25}$$

Thus, in the first approximation the reflection coefficient α_1 has the form

$$\alpha_1 = \frac{1-G}{1+G}, \quad G = 2\,\frac{\varepsilon_0}{\varepsilon}\,I_{11}\left(q_1^2 a^2 - a^2\frac{\omega^2\varepsilon}{c^2}\right)^{1/2}, \tag{26}$$

while all other coefficients vanish:

$$\alpha_n = 0 \quad (n \neq 1). \tag{27}$$

We also constructed the second approximation to the solution of system of equations (19) for the coefficients α_p. It was shown that the coefficient α_1 in the second approximation acquires only small corrections. Calculations were performed in a broad range of ratios of the aperture radius to the wavelength ($0 \leqslant ka \leqslant \xi_1 = 2.4048$). We established that the relative errors in calculations of the real $(\mathrm{Re}\,\alpha_1^{(2)} - \mathrm{Re}\,\alpha_1^{(1)})/\mathrm{Re}\,\alpha_1^{(2)}$ and imaginary $(\mathrm{Im}\,\alpha_1^{(2)} - \mathrm{Im}\,\alpha_1^{(1)})/\mathrm{Im}\,\alpha_1^{(2)}$ parts of the reflection coefficient found in the first approximation do not exceed 6 % and 5 %, respectively. As for the moduli of the coefficients at highest-order modes, they prove to be significantly lower than the modulus α_1. In this connection, we can assume that expression (26) obtained in the first approximation for the coefficient α_1 gives good approximation to the exact solution of the problem. This approximation will be used below to study the problem. Note here that according to general expressions (4)–(6) in the specified approximation, the time averaged energy densities of the electric [$(w^{\mathrm{el}} = (\varepsilon/16\pi)|\boldsymbol{E}|^2]$ and magnetic p[$w^{\mathrm{m}} = (\mu/16\pi)|\boldsymbol{H}|^2$, $\mu = 1$] field components at the waveguide output ($z = 0$) depending on the transverse coordinate ρ are determined for the TM_{01} mode by the expressions

$$w_\rho^{\mathrm{el}} = \frac{\varepsilon}{16\pi}\,|C|^2|1+\alpha_1|^2 J_1^2(q_1\rho),$$
$$w_z^{\mathrm{el}} = \frac{\varepsilon|C|^2|1-\alpha_1|^2 q_1^2 J_0^2(q_1\rho)}{16\pi(q_1^2 - \omega^2\varepsilon/c^2)}, \tag{28}$$

$$w_\varphi^{\mathrm{m}} = \left(\frac{\omega\varepsilon^{1/2}}{c}\right)^2 \frac{\varepsilon|C|^2|1-\alpha_1|^2 J_1^2(q_1\rho)}{16\pi(q_1^2 - \omega^2\varepsilon/c^2)}\,. \tag{29}$$

The dependences w_ρ^{el}, w_z^{el} and w_φ^{m} on the ratio ρ/a are presented in Fig. 2.

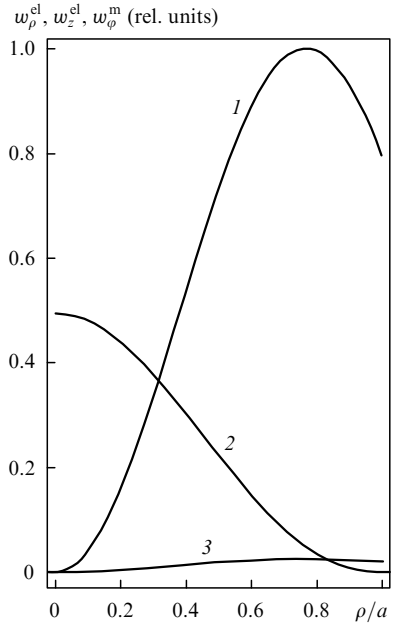

Figure 2. Energy densities of field components w_ρ^{el} (*1*), w_z^{el} (*2*), w_φ^{m} (*3*) at the cylindrical waveguide output ($z = 0$) as a function of the dimensionless transverse coordinate ρ/a. Calculations are performed for the waveguide mode TM_{01} at $\omega a\varepsilon_0^{1/2}/c = \pi/5$, $\varepsilon = 2.25$ and $\varepsilon_0 = 1$.

6. Reflection coefficient

Recall that the coefficient α_1 obtained in the previous section corresponds to the transformation of the initial evanescent TM_{01} mode to the reflected mode (having the same transverse structure and inverted dependence of the field on the coordinate z). In this case, the coefficients of the transformation to all other modes prove negligibly small. Thus, it is natural to call the α_1 coefficient the reflection coefficient. Note some of its properties. We will concentrate our attention on the case, when the dielectric constants ε and ε_0 are real and positive. It is obvious that at $\mathrm{Re}\,\alpha_1 \approx 1$ we deal with the antinode of the tangential electric-field component E_ρ at the waveguide output ($z = 0$) and the

node for the components E_z and H_φ [see (4)–(6)]. On the contrary, the value $\mathrm{Re}\,\alpha_1 \approx -1$ would correspond to the antinode of the components H_φ and E_z and the node for the component E_ρ. The imaginary part $\mathrm{Im}\,\alpha_1$ of the reflection coefficient is directly associated with the energy flux in the waveguide, and hence, to the flux in the far-field region (see section 7). Note that a simple asymptotic expression for the reflection coefficient follows from (22), (26) at small ka. In particular, for a hollow waveguide, at $\varepsilon = \varepsilon_0 = 1$ and $ka \ll 1$, we obtain

$$\mathrm{Re}\,\alpha_1 = 0.0724, \quad \mathrm{Im}\,\alpha_1 = -0.0551(ka)^3. \tag{30}$$

The characteristic dependences of the real and imaginary parts of the reflection coefficient α_1 of the evanescent wave ($0 \leqslant ka \leqslant \xi_1$) on the quantity ka are shown in Fig. 3 [curve (*1*)]. One can see that at $\varepsilon = \varepsilon_0 = 1$ the real part of the reflection coefficient weakly depends on ka in the entire subwavelength region up to $ka \sim 1$. Strong changes appear only at $ka \approx 1.5$, when the argument begins approaching the eigenvalues $\xi_1 = q_1 a$ of the TM_{01} mode. Unlike this, the imaginary part α_1 strongly changes with increasing ka already in the vicinity of the zero argument, achieves a minimum at $ka = 2.2$, and then increases and vanishes at $ka = \xi_1$.

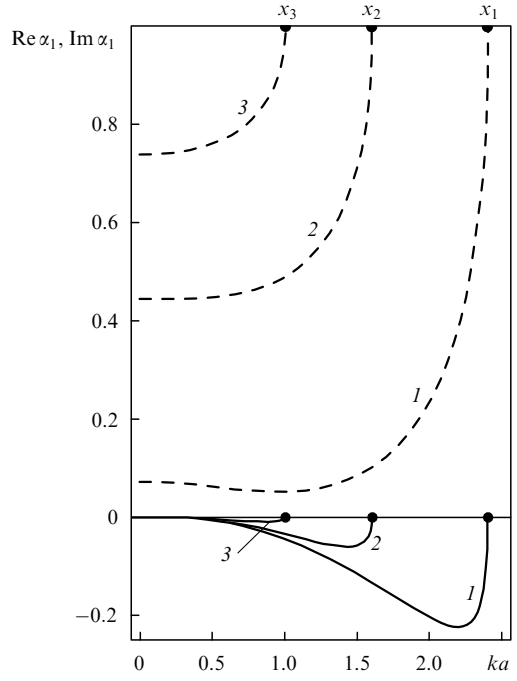

Figure 3. Real (dashed curves) and imaginary (solid curves) parts of the amplitude reflection coefficient α_1 of the evanescent wave from the output aperture of the nanowaveguide as a function of the quantity ka at $(\varepsilon/\varepsilon_0)^{1/2} = 1$ (*1*), 1.5 (*2*), 2.4 (*3*) and $\varepsilon_0 = 1$. The point numbers x_j ($j = 1 - 3$) correspond to the curve numbers.

The considered reflection coefficient of the evanescent TM_{01} wave from the subwavelength aperture of a hollow waveguide will be used in section 8 in discussing the dependence of the field parameters on the dielectric constant of the waveguide core.

7. Complex flw and an energy flux in a supercritical open waveguide

Obviously, a supercritical mode in an infinite cylindrical waveguide does not carry an energy flux. For an evanescent waveguide mode, complex amplitudes of tangential components of the electric and magnetic fields are shifted in phase by 90° so that the electromagnetic flow turns to be a purely imaginary quantity. At the same time, in the case of a truncated waveguide, the initial mode at its output is partially transformed into the reflected mode, which changes the phase relations between the total field components.

We will express the complex electromagnetic flow j at the output hole through the found reflection coefficient α_1. For the field under study (a monochromatic field with the components independent of the angular variable), the flow via an element of size πa^2 is expressed through a time-averaged complex Poynting vector $\boldsymbol{P}$ integrated over the surface (see, for example, [24, 25]):

$$j = 2\pi \int_0^a P_z \rho \mathrm{d}\rho, \quad \boldsymbol{P} = \frac{c}{8\pi} \boldsymbol{E} \times \boldsymbol{H}^*. \tag{31}$$

Let us use expressions for fields (4), (6) and, in accordance with the results of section 5, set in them $\alpha_n = 0$ at $n \neq 1$. By substituting these expressions into (31) and integrating them taking (18) into account, we obtain the expression for the flow. To emphasise the fact that in calculations, field components $\tilde{E}_\rho$ and $\tilde{H}_\varphi$ inside the waveguide are used, we will denote below the corresponding complex flow by $\tilde{j}$. The expression for $\tilde{j}$ has the form:

$$\tilde{j} = \frac{c}{4} \int_0^a \tilde{E}_\rho(\rho, 0) \tilde{H}_\varphi^*(\rho, 0) \rho \mathrm{d}\rho = \mathrm{i}\omega\varepsilon |C|^2 (1 + \alpha_1)(1 - \alpha_1^*)$$
$$\times a^3 J_1^2(\xi_1) \left[8 \left(\xi_1^2 - a^2 \frac{\omega^2 \varepsilon}{c^2} \right)^{1/2} \right]^{-1}. \tag{32}$$

The energy flux is determined by the real part of complex flow (32) and the expression for this energy flux has the form

$$\mathrm{Re}\,\tilde{j} = -\omega\varepsilon \frac{a^3}{4} |C|^2 J_1^2(\xi_1) \left(\xi_1^2 - a^2 \frac{\omega^2 \varepsilon}{c^2} \right)^{-1/2} \mathrm{Im}\,\alpha_1. \tag{33}$$

Expression (33) shows that in a truncated waveguide, the energy flux is nonzero only if the imaginary part of the reflection coefficient is nonzero. Thus, the energy flux in the waveguide and, hence, the flux to the far-field region are proportional to the imaginary part of the coefficient α_1. Recall that the real part α_1 is important for determining the field energy density in the near-field region. Thus, the coefficient α_1 is a very informative characteristic of the problem. It can serve as a basis for studying other types of nanowaveguides and other waveguide modes as well as for the further generalisation of the theory to the case of the walls of a waveguide made of real metal.

8. Dependence of the reflection coefficient on the dielectric constant and the value *ka*

We will discuss now the parameters of the amplitude reflection coefficient as functions of the dielectric constants of the waveguide core (ε) and the environment (ε_0) as well

as of the ratio of the aperture diameter to the radiation wavelength. The results of our calculations of the dependences of α_1 on ka at different ε are presented in Fig. 3. The dielectric constant of the free space outside the waveguide was assumed equal to unity ($\varepsilon_0 = 1$) and the refractive index of the waveguide core $n_w = \varepsilon^{1/2}$ was 1, 1.5 and 2.4. The latter two values of n_w correspond to the refractive indices of the optical fibre (or crystalline quartz) and silicon nitride. Therefore, the performed calculations are related to the applied problems on the near-field optical probes.

The curves presented in Fig. 3 show that the dependences of the real and imaginary parts of the reflection coefficient on ka for different ε have a qualitative resemblance. However, the specified values of $\mathrm{Re}\,\alpha_1$ and $\mathrm{Im}\,\alpha_1$ significantly differ from those obtained for $\varepsilon = 1$. In other words, the ratio $\varepsilon/\varepsilon_0$ strongly affects $\mathrm{Re}\,\alpha_1$ and $\mathrm{Im}\,\alpha_1$. It follows from the comparison of the curves that the quantity $\mathrm{Re}\,\alpha_1$ at the given ka strongly increases with increasing the ratio $\varepsilon/\varepsilon_0$. For example, in the region of small ka the real part of the amplitude reflection coefficient of the optical fibre and the silicon nitride exceeds that of the hollow waveguide by 6.1 and 10.2 times, respectively. Note also that the position of points on the ka axis at which $\mathrm{Re}\,\alpha_1$ achieves the unity and $\mathrm{Im}\,\alpha_1$ vanishes is determined by the quantities $x = ka = \xi_1(\varepsilon_0/\varepsilon)^{1/2}$, where $\xi_1 = 2.4048$. At the given x, the evanescent mode undergoes a transformation to the propagating one. Figure 3 shows the points (x_1, x_2 and x_3) for three values of the dielectric constant ε.

One can see from Fig. 3 that at large $\varepsilon/\varepsilon_0$, the real part of the reflection coefficient becomes close to unity. At the waveguide output, this differently affects the energy density, which is caused by the different field components. For the TM_{01} mode under study, the energy density w_ρ^{el} [see (28)] associated with the transverse electric-field component E_ρ and proportional to $|1 + \alpha_1|^2$ can increase by approximately four times compared to its value in the unperturbed waveguide. At the same time, the energy densities of the magnetic field H_φ and longitudinal electric-field components E_z, which are proportional to $|1 - \alpha_1|^2$ [see (28) and (29)], tend to zero at $\alpha_1 \to 1$. These peculiarities in the behaviour of different field components of the energy density are shown in Fig. 4. This figure presents the calculation results of the dependences of $|1 + \alpha_1|^2$ and $|1 - \alpha_1|^2$ on ka for a hollow waveguide ($n_w = 1$) and the silicon nitride core ($n_w = 2.4$) as well as for waveguides made of silicon, which is a highly refractive semiconductor material ($n_w = 3.5$). It follows from the calculations that the main (at $ka \ll 1$) contribution to the integral energy density ($W_\rho = 2\pi \int_0^a w_\rho^{el} \rho \mathrm{d}\rho$) is affected by both the reflection from the output aperture and by the decrease in the decay in the supercritical waveguide at a large dielectric constant of its core [19–21]. Figure 4 shows the points $x_1 - x_4$ at which the evanescent mode is transformed into a propagating mode for four ε.

Note that our approach remains valid for negative values of the dielectric constant of the environment ($\varepsilon_0 < 0$). In this case, we observe an interesting feature in the behaviour of the reflection coefficient. From the physical point of view, the negative value of $\varepsilon_0/\varepsilon$ corresponds to the metal medium at the waveguide output for the positive dielectric constant of the waveguide core ($\varepsilon > 0$). According to general expression (26), when $G = -1$, a singularity appears in the behaviour of α_1. This phenomenon is demonstrated in Fig. 5, which presents the calculation

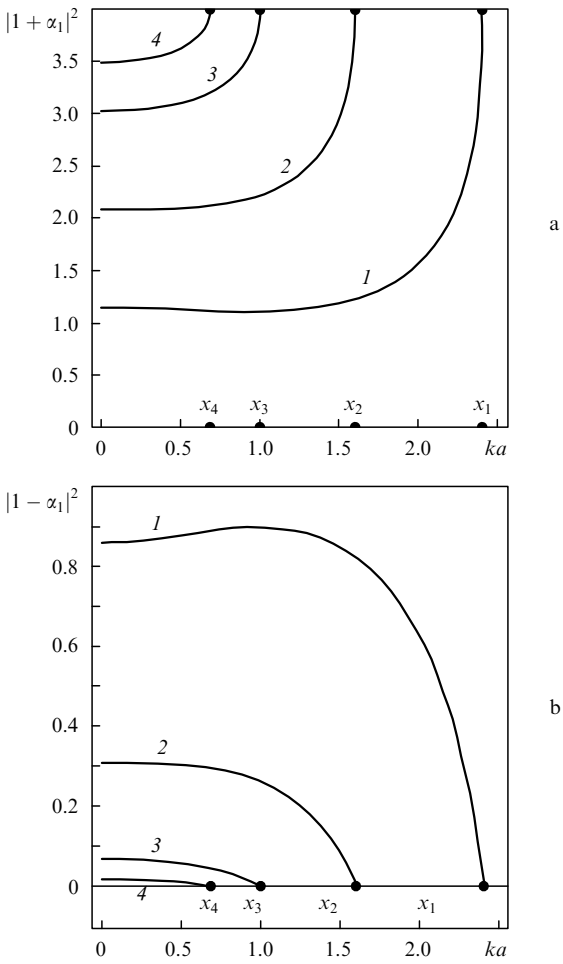

Figure 4. ka dependences of the factor $|1 + \alpha_1|^2$ determining the ratio of the square of modulus of the transverse electric-field component $|E_\rho|^2$ (perturbed by the reflection from the subwavelength aperture of the truncated waveguide) to the corresponding value $|E_\rho^{(0)}|^2$ in a waveguide of infinite length (a) and of the factor $|1 - \alpha_1|^2$ determining the influence of the subwavelength aperture on the square of modulus of the longitudinal electric-field component and the transverse magnetic-field component ($|E_z/E_z^{(0)}|^2$, $|H_\varphi/H_\varphi^{(0)}|^2 \propto |1 - \alpha_1|^2$) (b) at $(\varepsilon/\varepsilon_0)^{1/2} = 1$ (*1*), 1.5 (*2*), 2.4 (*3*) and $\varepsilon_0 = 1$. The point numbers x_j ($j = 1 - 4$) correspond to the curve numbers.

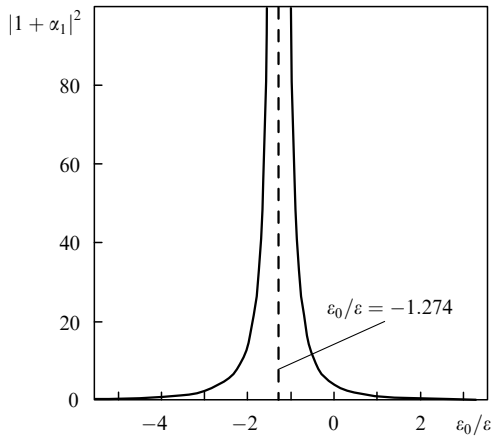

Figure 5. Dependence of the square of modulus of the transverse electric-field component reflected from the subwavelength aperture of a truncated waveguide ($|E_\rho/E_\rho^{(0)}|^2 \propto |1 + \alpha_1|^2$) on the ratio of the electric constants of the environment to the waveguide core, $\varepsilon_0/\varepsilon$, calculated at the fixed parameter $\omega a \varepsilon^{1/2}/c = \pi/5$.

results of the real part of the reflection coefficient α_1 as a function of the ratio $\varepsilon_0/\varepsilon$. The calculations were performed for the fixed positive dielectric constant ε of the waveguide core and for the given ratio $a\omega\varepsilon^{1/2}/c = \pi/5$. Recall that the real part of the coefficient α_1 is not related to the energy flux. The increase in $\mathrm{Re}\,\alpha_1$ means an increase in the energy density of the transverse electric-field component E_ρ in the near-field region at the waveguide output. The imaginary part of α_1 is equal to zero at $\varepsilon_0/\varepsilon < 0$. Thus, in the case under study the energy flux and the transmission coefficient of light in the far-field region are equal to zero because both these quantities are proportional to $\mathrm{Im}\,\alpha_1$.

One can see from Fig. 5 that the singularity in the behaviour of $\mathrm{Re}\,\alpha_1$ appears at $\varepsilon_0/\varepsilon = -1.274$. This singularity leads to a drastic increase in the amplitude (and, hence, in the energy density) of the transverse electric-field component $E_\rho \propto (1+\alpha_1)$ as ε_0/ϵ is approached to the specified resonance value. In a waveguide with a glass-optical core ($n_w = 1.5$), the resonance appears at the dielectric constant of the external medium $\varepsilon_0 = -2.866$. Taking into account the specific type of the dependences of dielectric constants in Ag and Au on the wavelength in vacuum [26], we obtain that the resonance increase in the field for Ag and Au occurs at $\lambda = 370$ and 505 nm, respectively.

Note that in our example the real part of the reflection coefficient $\mathrm{Re}\,\alpha_1$ tends to infinity because we consider a dissipationless medium at the waveguide output. When the imaginary part of the dielectric constant in metal is taken into account, we will simply obtain a drastic (resonance) increase in the field amplitude instead of the singularity. This effect is similar to other effects of the plasmon resonance (appearing at the metal–dielectric medium interface), which in recent years have been actively discussed in many papers on nanooptics (see review [27]). The detailed analysis of the effects of the resonance reflection of evanescent waves from a metal substrate at the nanowaveguide output will be studied elsewhere.

9. Application of the boundary condition for the complex flow to waveguide problems

The formulated problem was studied by using Maxwell's equations and exact boundary conditions for the fields. When deriving system of equations (19) we did not use any approximations. After system (19) was derived, we constructed its solution in the first and second approximations and showed that these solutions differ insignificantly. On this basis we selected equality (26) as a working expression. Recall that this result directly followed from equality (24) representing an initial equation in the first approximation. We will show how this equality can be interpreted. By multiplying both parts of (24) by the factor $-\mathrm{i}\omega CC^*(1+\alpha_1^*)J_1^2(q_1a)a^3/8$ we pass to the complex-conjugate quantities. It turns out that the left-hand side of the equality is exactly equal to the product of the factor $c/4$ by the integral

$$\int_0^a \tilde{E}_\rho(\rho,0)\tilde{H}_\varphi^*(\rho,0)\rho\mathrm{d}\rho,$$

and the right-hand side – the product of $c/4$ by the integral

$$\int_0^a E_\rho(\rho,0)H_\varphi^*(\rho,0)\rho\mathrm{d}\rho.$$

These products coincide with the expressions for the complex light flow integrated in the aperture [see definition (31)]. In this case, the left-hand side includes the integrated flow expressed through the fields related to the waveguide and the right-hand side – through the fields in the external space (the flows are denoted by $\tilde{j}$ and j). Thus equation (24) represents the equality of integral complex flows calculated at $z = -0$ and $z = +0$:

$$\tilde{j} = j. \tag{34}$$

It is obvious that if the continuity condition is fulfilled for tangential components of the electric and magnetic fields at the boundary $z = 0$, equality (34) is fulfilled as well. However, the continuity of the tangential component of the magnetic field at all the points of the output aperture does not follow from the tangential component of the electric field and condition (34), i.e. condition (34) is weaker than the exact boundary condition for the magnetic field. The equivalence of relations (24) and (34) means that if in the case under study we replaced, at the beginning, the exact boundary condition for the tangential magnetic-field component by approximate condition (34), we arrived at the same result given by the solution of the exact system of equations in the first approximation. This allows us to draw a conclusion that in many more complicated waveguide problems (other types of waveguide modes, an open waveguide of the variable cross section, the case of nonideal metal on the walls) we can use the equality condition for the integral complex flows at the interface instead of the continuity condition of the tangential magnetic-field component at each point. This approach promises significant simplification of the procedure of the solution construction for the above problems.

10. Conclusions

Let us formulate the results of the paper:

(i) we have developed a theoretical approach to the investigation of a spatial structure of evanescent fields in the truncated waveguide and the surrounding open space. We have shown that in the supercritical waveguide the waveguide mode is transformed mainly to the mode with the transverse structure and inverted dependence on the longitudinal coordinate.

(ii) We have introduced the reflection coefficient for the initial evanescent wave. We have obtained the dependence on the waveguide radius, the wavelength and dielectric constant of the waveguide and the free space. It has been shown that the reflection coefficient is a small quantity, if the dielectric constant is continuous at the waveguide–free space interface. The jump of the dielectric constant strongly increases the amplitude of the reflected wave and the field near the output hole of the waveguide.

(iii) The increase in the ratio $\varepsilon/\varepsilon_0$ of the dielectric constants in the waveguide core (ε) and environment (ε_0) results in a significant increase in the real part of the reflection coefficient α_1 and the increase in the field energy density in the near-field region. The quantity α_1 approaches unity at large $\varepsilon/\varepsilon_0$, which ensures a four-fold increase in the energy density of the transverse electric-field component $w_\rho^{\mathrm{el}} \propto |1+\alpha_1|^2$ compared to the case of the unperturbed waveguide of infinite length. This indicates the additional advantage in the use of near-field optical probes with a large

dielectric constant of the core, i.e. the effect acts as the decrease in the decay length of evanescent waves in a supercritical tapered waveguide [19 – 22].

(iv) It is shown that in the case of a medium with a negative dielectric constant at the waveguide output, the reflected wave amplitude resonantly increases at certain frequencies. This is a consequence of excitation of surface plasmons and can serve as an effective instrument for measuring metal properties of the object under study, which is placed at the probe output.

(v) The main calculations have been performed for transverse-magnetic modes. However, the theory allows generalisation to the case of transverse-electric modes and to the case of tapered waveguides, which are of special interest for the near-field microscopy. The important moment consists in the possibility of generalisation of the proposed approach to the case of nanowaveguides with a real metal coating, which is the subject of our next paper.

Acknowledgements. This work was supported by the Russian Foundation for Basic Research (Grant Nos 09-02-01024 and 07-02-00873), the 'Development of the Scientific Potential of the Higher School' program (Project No. 2.1.1/4294) and by programs 'Optical Spectroscopy and Frequency Standards' and 'Coherent Optical radiation of Semiconductor Compounds and Structures' of the Department of Physical Sciences, RAS.

References

1. Pohl D.W. *Philos. Trans. R. Soc. London A*, **362**, 701 (2004).
2. Garcia de Abajo F.J. *Rev. Mod. Phys.*, **79**, 1267 (2007).
3. Bethe H.A. *Phys. Rev.*, **66**, 163 (1944).
4. Bouwkamp C.J. *Rep. Prog. Phys.*, **17**, 35 (1954).
5. Roberts A. *J. Opt. Soc. Am. A*, **11**, 1970 (1987).
6. Roberts A. *J. Appl. Phys.*, **70**, 4045 (1991).
7. Novotny L., Pohl D.W., Regli P. *J. Opt. Soc. Am. A*, **11**, 1768 (1994).
8. Knoll B., Keilman F. *Opt. Commun.*, **162**, 177 (1999).
9. Drezet A., Woehl J.C., Huant S. *Phys. Rev. E*, **65**, 046611 (2002).
10. Alvarez L., Sauceda A., Xiao M. *Opt. Commun.*, **219**, 9 (2003).
11. Garcia de Abajo F.J. *Opt. Express*, **10**, 1475 (2002).
12. Lezec H.J., Thio T. *Opt. Express*, **12**, 3629 (2004).
13. Olkkonen J., Kataja K., Howe D.G. *Opt. Express*, **13**, 6980 (2005).
14. Garcia-Vidal F.J., Moreno E., Porto J.A., Martin-Moreno L. *Phys. Rev. Lett.*, **95**, 103901 (2005).
15. Webb K.J., Li J. *Phys. Rev. B*, **73**, 033401 (2006).
16. Kuznetsova T.I., Lebedev V.S. *Kvantovaya Elektron.*, **32**, 727 (2002) [*Quantum Electron.*, **32**, 727 (2002)].
17. Kuznetsova T.I., Lebedev V.S. *Kvantovaya Elektron.*, **33**, 931 (2003) [*Quantum Electron.*, **33**, 931 (2003)].
18. Kuznetsova T.I., Lebedev V.S., Tsvelik A.M. *J. Opt. A: Pure Appl. Opt.*, **6**, 338 (2004).
19. Kuznetsova T.I., Lebedev V.S. *Pis'ma Zh. Eksp. Teor. Fiz.*, **79**, 70 (2004) [*JETP Lett.*, **79**, 62 (2004)].
20. Kuznetsova T.I., Lebedev V.S. *Kvantovaya Elektron.*, **34**, 361 (2004) [*Quantum Electron.*, **34**, 361 (2004)].
21. Kuznetsova T.I., Lebedev V.S. *Phys. Rev. B*, **70**, 035107 (2004).
22. Lebedev V.S., Kuznetsova T.I., Vitukhnovskii A.G. *Dokl. Ros. Akad. Nauk.*, **410**, 749 (2006) [*Dokl. Phys.*, **51**, 542 (2006)].
23. Vainshtein L.A. *The Theory of Diffraction and the Factorization Method* (Boulder, Colo.: Golem Press, 1969; Moscow: Sov. radio, 1966).
24. Vainshtein L.A. *Elektromagnitnye volny* (Electromagnetic Waves) (Moscow: Radio i svyaz', 1988).
25. Jackson J.D. *Classical Electrodynamics* (New York: Wiley, 1962; Moscow: Mir, 1965).
26. Johnson P.B., Christy R.W. *Phys. Rev. B*, **6**, 4370 (1972).
27. Barnes W.L. *J. Opt. A: Pure Appl. Opt.*, **8**, 87 (2006).